



北京航空航天大学
BEIHANG UNIVERSITY

Measurements of Born Cross Section of $e^+e^- \rightarrow D_s D_{s1}(2460)$ and $e^+e^- \rightarrow D_s^* D_{s1}(2460)$

TianYu Qi

July 10, 2018

Table of Content

- 1 Motivation
- 2 Dataset
- 3 Common Selection Criteria
- 4 The Study of $e^+ e^- \rightarrow D_s^+ D_{s1}^- (2460)$
 - Special Event Selection
 - Background Analysis
 - Fit of MC and Data
- 5 Tagging π^0 in $D_{s1} (2460) \rightarrow \pi^0 + anything$
 - Special Event Selection
 - Fit of MC and Data
- 6 The Study of $e^+ e^- \rightarrow D_s^{*+} D_{s1}^- (2460)$
 - Special Event Selection
 - Background Analysis
 - Fit of MC and Data
- 7 Summary



Motivation

- 1 $D_{s1}(2460)$, first observed in 2003 by CLEO[1] and Belle[2] Collaborations via $D_s \pi^0 \gamma$, and subsequently confirmed by BaBar Collaboration[3].
- 2 Could be one of the missing $c\bar{s} 1^+$ state.
- 3 However, its mass is $(2459.5 \pm 0.6) \text{ MeV}/c^2$, lower than the prediction, and its width is unexpectedly narrow.
- 4 Also, can be a good candidate for D^*K molecule state[4, 5, 6], or a mixture of $c\bar{s}$ and D^*K state[7].

Motivation

- 1 $D_{s1}(2460)$, first observed in 2003 by CLEO[1] and Belle[2] Collaborations via $D_s \pi^0 \gamma$, and subsequently confirmed by BaBar Collaboration[3].
- 2 Could be one of the missing $c\bar{s} 1^+$ state.
- 3 However, its mass is $(2459.5 \pm 0.6) \text{ MeV}/c^2$, lower than the prediction, and its width is unexpectedly narrow.
- 4 Also, can be a good candidate for D^*K molecule state[4, 5, 6], or a mixture of $c\bar{s}$ and D^*K state[7].

Ref. [8] predicts that the cross section of two D_s channel should follow the excitation behavior for S wave production:

$$\sigma[e^+e^- \rightarrow D_{s0}^*(2317)D_s^*] = \sigma[e^+e^- \rightarrow D_s D_{s1}(2460)] \propto \sqrt{E_{cm} - E_0}$$

$E_{cm} = \sqrt{s}$, and $E_0 \approx 4.43 \text{ GeV}$ is the threshold of both channel. It also suggests to test it on BESIII.



Analysis Strategy

In this analysis, We can reconstruct D_s^\pm from $D_s^\pm \rightarrow K^+ K^- \pi^\pm$, and reconstruct $D_s^{*\pm}$ from $D_s^{*\pm} \rightarrow \gamma D_s^\pm$. Then, we will observe $D_{s1}(2460)$ in the D_s and D_s^* recoil spectrum.



Analysis Strategy

In this analysis, We can reconstruct D_s^\pm from $D_s^\pm \rightarrow K^+ K^- \pi^\pm$, and reconstruct $D_s^{*\pm}$ from $D_s^{*\pm} \rightarrow \gamma D_s^\pm$. Then, we will observe $D_{s1}(2460)$ in the D_s and D_s^* recoil spectrum. From now on, the charge conjunction channel will be included by default, unless pointed out explicitly.



Analysis Strategy

In this analysis, We can reconstruct D_s^\pm from $D_s^\pm \rightarrow K^+ K^- \pi^\pm$, and reconstruct $D_s^{*\pm}$ from $D_s^{*\pm} \rightarrow \gamma D_s^\pm$. Then, we will observe $D_{s1}(2460)$ in the D_s and D_s^* recoil spectrum. From now on, the charge conjugation channel will be included by default, unless pointed out explicitly.

For the study of $e^+ e^- \rightarrow D_s^+ D_{s1}^- (2460)$, in order to lower the background, we divide the D_s recoil spectrum into bins, and fit the D_s invariant mass spectrum in each bin. Then, we use the event count from the fit result to form and fit a D_s recoil spectrum from what we considered as real D_s event, and then get the $D_{s1}(2460)$ count.



Dataset

Data Point

$e^+e^- \rightarrow D_s D_{s1}(2460)$ at four data points above $\sqrt{s} \geq 4.467$ GeV.

$e^+e^- \rightarrow D_s^* D_{s1}(2460)$ at $\sqrt{s} = 4.575, 4.600$ GeV.

Dataset

Data Point

$e^+e^- \rightarrow D_s D_{s1} (2460)$ at four data points above $\sqrt{s} \geq 4.467$ GeV.

$e^+e^- \rightarrow D_s^* D_{s1} (2460)$ at $\sqrt{s} = 4.575, 4.600$ GeV.

BOSS version 7.0.3

Dataset

Data Point

$e^+e^- \rightarrow D_s D_{s1} (2460)$ at four data points above $\sqrt{s} \geq 4.467$ GeV.

$e^+e^- \rightarrow D_s^* D_{s1} (2460)$ at $\sqrt{s} = 4.575, 4.600$ GeV.

BOSS version 7.0.3

MC simulations

Create MC samples of these two channels,
with $D_s^{*+} \rightarrow \gamma D_s^+$, $D_s^+ \rightarrow K^+ K^- \pi^+$.

$D_{s1}^- (2460)$ decays inclusively.

The sixth comes from $\Gamma(D_{s1} (2460) \rightarrow \gamma D_s) / \Gamma(D_{s1} (2460) \rightarrow \gamma D_s^*)$ in Ref.[9].

ISR by KKMC.

Inclusive MC at $\sqrt{s} = 4.575, 4.600$ GeV
under BOSS 6.6.5p01 are used.

$$\begin{aligned}
 D_{s1}^- (2460) &\rightarrow \pi^0 D_s^{*-} & B &= 0.638 \\
 &\rightarrow \gamma D_s^- & B &= 0.18 \\
 &\rightarrow \pi^+ \pi^- D_s & B &= 0.043 \\
 &\rightarrow \gamma D_{s0}^{*-} (2317) & B &= 0.037 \quad (1) \\
 &\rightarrow \pi^0 \pi^0 D_s^- & B &= 0.022 \\
 &\rightarrow \gamma D_s^{*-} & B &= 0.08 \\
 D_{s0}^* (2317) &\rightarrow \pi^0 D_s & B &= 1.0
 \end{aligned}$$

Dataset

The cross section inputted is shown below, comes from rough measurement of cross section at four points. Use Gaussian for interpolation.

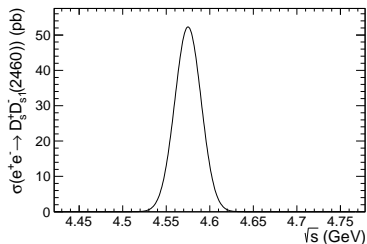


Figure: Cross section inputted for computing Initial State Radiation(ISR)

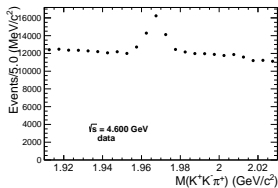
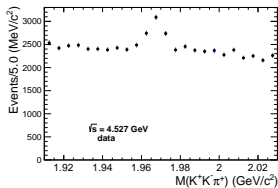
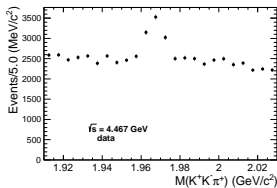
Selection Criteria

Basic selection

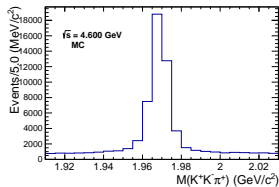
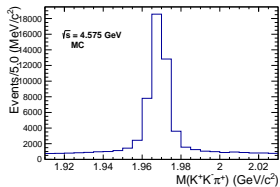
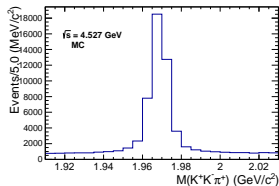
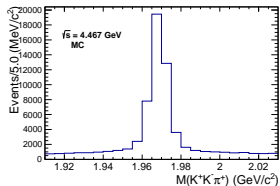
- 1 Charged Track: Begin from the interaction point, $V_{xy} < 1\text{cm}$, $|V_z| < 10\text{cm}$, and lie in $|\cos\theta| < 0.93$.
- 2 Neutral track:
 - 1 Deposit energy > 25 MeV in barrel EMC ($|\cos\theta| < 0.8$), > 50 MeV in end-cap EMC ($0.86 < |\cos\theta| < 0.92$).
 - 2 Angle between this track and the nearest charged track larger than 20 degree.
 - 3 Time information from EMC: $0 < t < 14$ (50ns).
- 3 Use PID to separate Kaon and pion: If $Prob(K) > Prob(\pi)$ and $Prob(K) > 0.001$, it is considered as Kaon. On the contrary, it is considered as pion.

$$e^+ e^- \rightarrow D_s^+ D_{s1}^- (2460) + c.c.$$

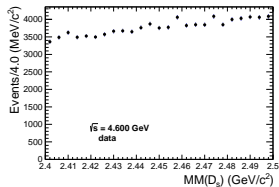
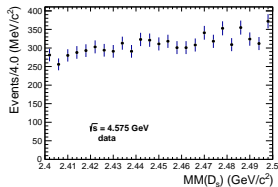
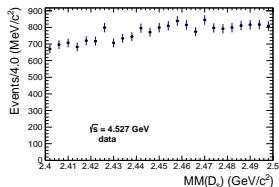
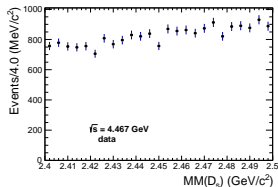
Require at least three good charged tracks. Perform a vertex fit.



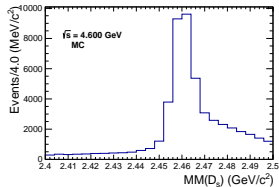
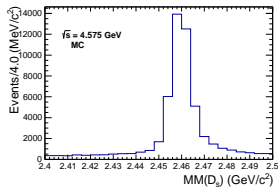
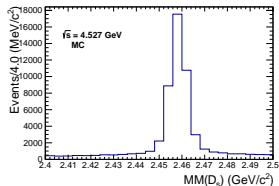
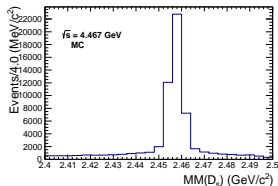
$$e^+ e^- \rightarrow D_s^+ D_{s1}^- (2460) + c.c.$$



$$e^+ e^- \rightarrow D_s^+ D_{s1}^- (2460) + c.c.$$



$$e^+ e^- \rightarrow D_s^+ D_{s1}^- (2460) + c.c.$$



Inclusive MC sample

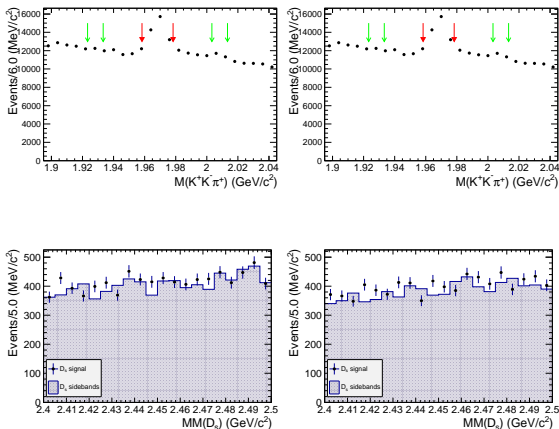


Figure: The D_s recoil mass spectrum only with D_s mass window cut, along with D_s sidebands.

Inclusive MC sample

We use the method stated before, fit entire D_s invariant mass spectrum, fix the signal shape, and fit the $M(D_s)$ in each bin.

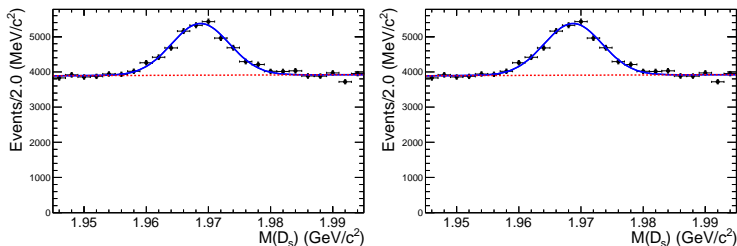


Figure: Fit the entire D_s invariant mass spectrum, for inclusive MC simulation at 4.575 GeV(left) and 4.600 GeV(right).

Inclusive MC sample

We use the method stated before, fit entire D_s invariant mass spectrum, fix the signal shape, and fit the $M(D_s)$ in each bin.

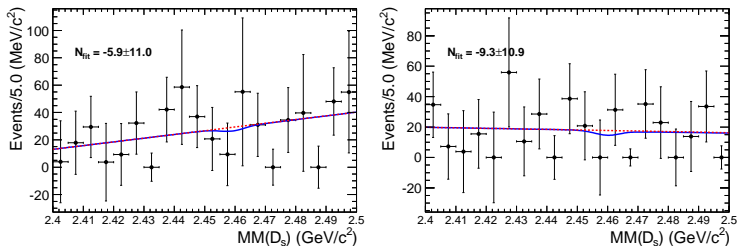


Figure: Divide the D_s recoil mass spectrum into bins, fit D_s invariant mass spectrum in each bin to get the real D_s event count, and then fit the D_s recoil mass spectrum, for inclusive MC simulation at 4.575 GeV(left) and 4.600 GeV(right).

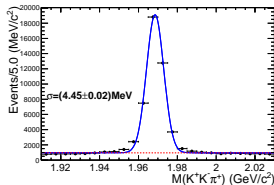
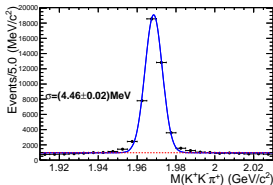
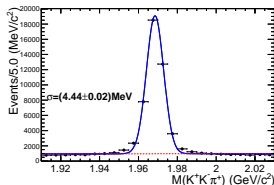
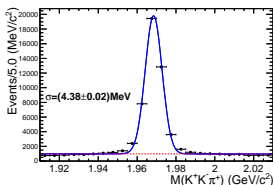
Background for $e^+e^- \rightarrow D_s^+ D_{s1}^- (2460)$

Potential backgrounds are listed below:

index	event tree	nEvts
1	$e^+e^- \rightarrow \pi^+ D^- D^{*0}, D^- \rightarrow \pi^- \pi^- K^+, D^{*0} \rightarrow \pi^0 D^0, D^0 \rightarrow \pi^0 \pi^+ K^-$	10
2	$e^+e^- \rightarrow \pi^+ \bar{D}^{*-} D^0, \bar{D}^{*-} \rightarrow \pi^- \bar{D}^0, D^{*0} \rightarrow \pi^0 D^0, \bar{D}^0 \rightarrow \pi^0 \pi^- K^+, D^0 \rightarrow \pi^0 \pi^+ K^-$	9
3	$e^+e^- \rightarrow \pi^- D^{*+} \bar{D}^0, D^{*+} \rightarrow \pi^+ D^0, \bar{D}^0 \rightarrow \pi^0 \pi^- K^+, D^0 \rightarrow \pi^0 \pi^+ K^-$	8
4	$e^+e^- \rightarrow \pi^- D^+ \bar{D}^{*0}, D^+ \rightarrow \pi^+ \pi^+ K^-, \bar{D}^{*0} \rightarrow \pi^0 \bar{D}^0, \bar{D}^0 \rightarrow \pi^0 \pi^- K^+$	8
5	$e^+e^- \rightarrow \pi^- D^{*+} \bar{D}^0, D^{*+} \rightarrow \pi^+ D^0, \bar{D}^0 \rightarrow \pi^0 \pi^- K^+, D^0 \rightarrow K^- a_1^+, a_1^+ \rightarrow \rho^0 \pi^+, \rho^0 \rightarrow \pi^+ \pi^-$	8
6	$e^+e^- \rightarrow \bar{D}^0 D^{*0}, \bar{D}^0 \rightarrow \pi^0 \pi^- K^+, D^{*0} \rightarrow D^0 \gamma, D^0 \rightarrow \pi^0 \pi^+ K^-$	8
7	$e^+e^- \rightarrow \pi^+ D^- D^{*0}, D^- \rightarrow \pi^- \pi^- K^+, D^{*0} \rightarrow D^0 \gamma, D^0 \rightarrow \pi^0 \pi^+ K^-$	7
8	$e^+e^- \rightarrow D^0 \bar{D}^{*0}, D^0 \rightarrow \pi^0 \pi^+ K^-, \bar{D}^{*0} \rightarrow \pi^0 \bar{D}^0, \bar{D}^0 \rightarrow \pi^0 \pi^- K^+$	7
9	$e^+e^- \rightarrow D^+ \bar{D}^{*-}, D^+ \rightarrow \mu^+ \nu_\mu K^*, \bar{D}^{*-} \rightarrow \pi^- \bar{D}^0, K^* \rightarrow \pi^+ K^-, \bar{D}^0 \rightarrow \pi^0 \pi^- K^+$	7
10	$e^+e^- \rightarrow \pi^- D^{*+} \bar{D}^0, D^{*+} \rightarrow \pi^+ D^0, \bar{D}^0 \rightarrow e^- \bar{\nu}_e K^+, D^0 \rightarrow K^- a_1^+, a_1^+ \rightarrow \rho^0 \pi^+, \rho^0 \rightarrow \pi^+ \pi^-$	7
11	$e^+e^- \rightarrow \pi^- D^+ \bar{D}^{*0}, D^+ \rightarrow \pi^+ \pi^+ K^-, \bar{D}^{*0} \rightarrow \pi^0 \bar{D}^0, \bar{D}^0 \rightarrow K^+ a_1^-, a_1^- \rightarrow \rho^0 \pi^-, \rho^0 \rightarrow \pi^+ \pi^-$	6
12	$e^+e^- \rightarrow \pi^+ \bar{D}^{*-} D^0, \bar{D}^{*-} \rightarrow \pi^- \bar{D}^0, D^0 \rightarrow \pi^0 \pi^+ K^-, \bar{D}^0 \rightarrow \pi^0 \pi^- K^+$	6
13	$e^+e^- \rightarrow \pi^0 D^- D^{*+}, D^- \rightarrow \pi^- \pi^- K^+, D^{*+} \rightarrow \pi^+ D^0, D^0 \rightarrow \pi^0 \pi^+ K^-$	6
14	$e^+e^- \rightarrow \pi^- D^+ \bar{D}^{*0}, D^+ \rightarrow \pi^+ \pi^+ K^-, \bar{D}^{*0} \rightarrow \pi^0 \bar{D}^0, \bar{D}^0 \rightarrow e^- \bar{\nu}_e K^+$	6
15	$e^+e^- \rightarrow D_s^+ D_s^{*-}, D_s^+ \rightarrow \pi^+ K^+ K^-, D_s^{*-} \rightarrow D_s^- \gamma, D_s^- \rightarrow \pi^- K^+ K^-$	6
16	$e^+e^- \rightarrow \pi^- D^+ \bar{D}^{*0}, D^+ \rightarrow \pi^+ \pi^+ K^-, \bar{D}^{*0} \rightarrow \bar{D}^0 \gamma, \bar{D}^0 \rightarrow \pi^0 \pi^- K^+$	6

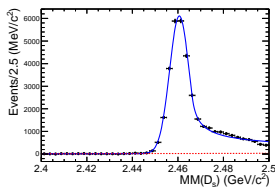
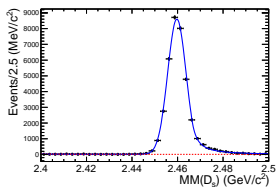
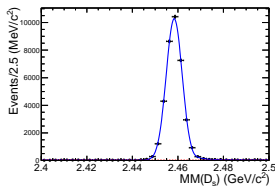
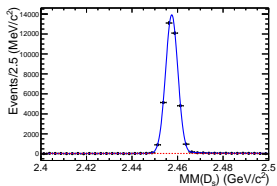
Fit of MC Simulation

First, fit the entire D_s invariant mass spectrum. Gaussian for signal, and 1st order polynomial for background. Then, fix the signal shape and fit the D_s invariant mass spectrum in each bin.



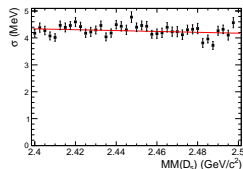
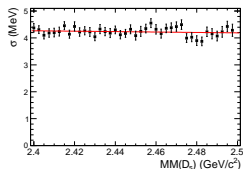
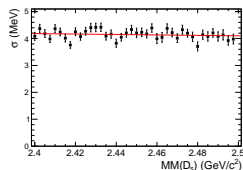
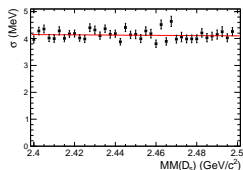
Fit of MC Simulation

After that, fit D_s recoil mass spectrum. Crystal ball for signal, 1st order polynomial for background.



Test Whether Resolution Varies

We perform a special MC simulation, where the width of $D_{s1}^- (2460)$ is set to 500 MeV, to ensure that we get enough events in each $MM(D_s)$ bin. Decay chain unchanged. Then, use the technique above to fit this sample; plot and linear fit the $\sigma - MM(D_s)$ spectrum from the fitting in each bin.



Fit of Data

After fitting the MC simulation, we perform the same fit for data.

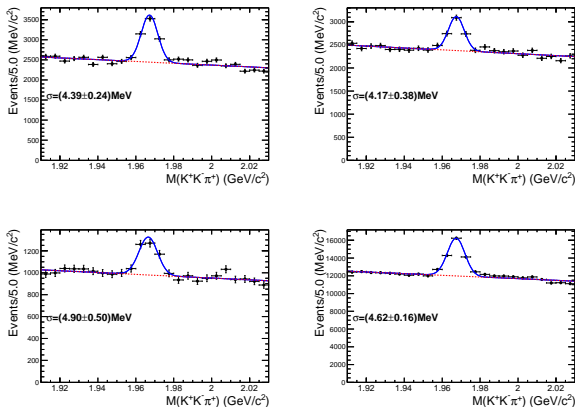
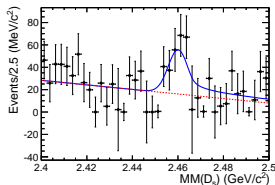
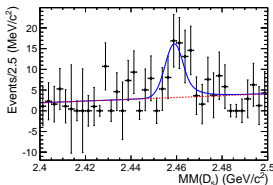
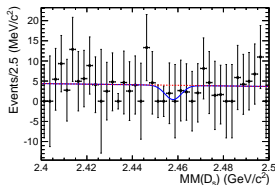
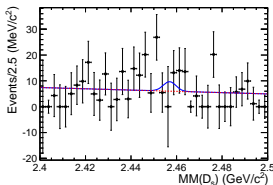


Figure: Fit the entire D_s invariant mass spectrum.

Fit of Data

Crystal ball convolve Gaussian for signal, where the Gaussian function represents the difference between data and MC on resolution and its σ is fixed to 0.9MeV. The shape of the Crystal ball function is fixed to the MC sample.



Fit Result

center-of-mass energy	efficiency	N_{event}	$(1 + \delta)^{ISR}$	significance
4.467	37.4%	10.4 ± 7.4	1.035	1.5σ
4.527	36.4%	-13.0 ± 2.6	0.687	—
4.575	38.6%	49.3 ± 9.0	0.715	7.5σ
4.600	35.3%	218.6 ± 24.6	1.053	11.9σ

Table: N_{event} come from data fitting and efficiency come from MC simulation. Errors here are statistical only.

Born Cross Section

$$\sigma = \frac{N_{obs}}{(1 + \delta)^{VP} * \epsilon_{D_s} * B(D_s \rightarrow K^+ K^- \pi) * L * (1 + \delta)^{ISR}} \quad (2)$$

- N_{obs} stands for the number of events come from fitting data;
- ϵ_{D_s} stands for the D_s detect efficiency;
- $B(D_s \rightarrow K^+ K^- \pi)$ stands for the branch fraction of $D_s^\pm \rightarrow K^+ K^- \pi^\pm$, which equals to 5.45% according to PDG[10];
- L stands for the integrated luminosity at each energy point;
- $(1 + \delta)^{VP}$ stands for vacuum polarization factor, which equals to 1.055 at all four energy point[11];
- $(1 + \delta)^{ISR}$ stands for initial state radiation correction factor, which can be read from KKMC.

Born Cross Section

energy point	σ
4.467	$4.2 \pm 3.0\text{pb}$
4.527	$-8.1 \pm 1.6\text{pb}$
4.575	$65.37 \pm 11.9\text{pb}$
4.600	$17.4 \pm 2.0\text{pb}$

Table: Born cross section of $e^+e^- \rightarrow D_s D_{s1}(2460)$ calculated at four energy point

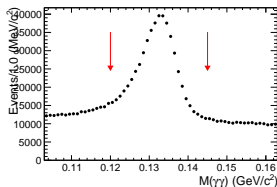
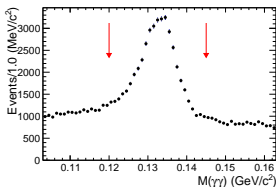
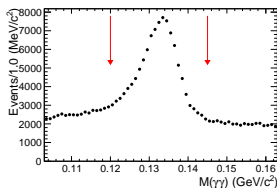
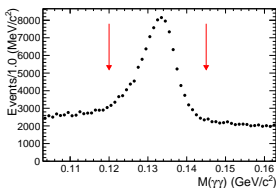
It will be plotted later.

π^0 Tag

To decrease the background, we try tagging π^0 in the $D_{s1}(2460)$ decay product, which is actually, measuring the cross section of $e^+e^- \rightarrow D_s D_{s1}(2460), D_{s1}(2460) \rightarrow \pi^0 + \text{anything}$.

π^0 Tag

To decrease the background, we try tagging π^0 in the $D_{s1}(2460)$ decay product, which is actually, measuring the cross section of $e^+e^- \rightarrow D_s D_{s1}(2460), D_{s1}(2460) \rightarrow \pi^0 + \text{anything}$.



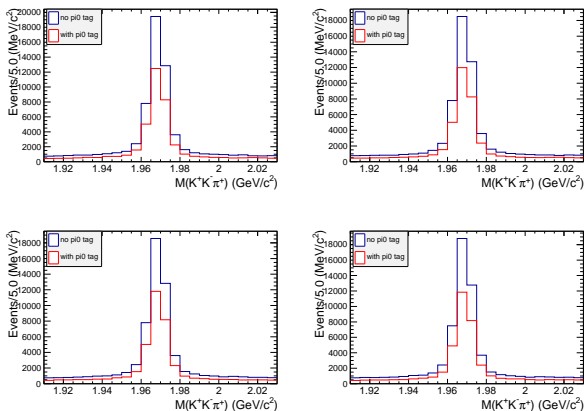
π^0 Tag

Figure: The entire D_s invariant mass spectrum with and without π^0 tag, for MC at 4.467 GeV (upper left), 4.527 GeV (upper right), 4.575 GeV (lower left) and 4.600 GeV (lower right).

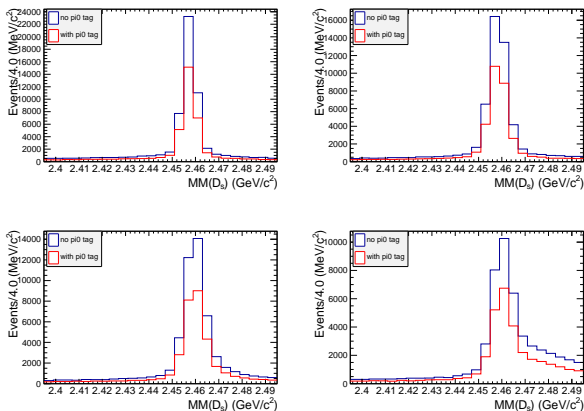
π^0 Tag

Figure: The D_s recoil mass spectrum with and without π^0 tag, for MC at 4.467 GeV(upper left), 4.527 GeV(upper right), 4.575 GeV(lower left) and 4.600 GeV(lower right).

π^0 Tag

The $D_{s1}^- (2460)$ in the signal MC sample here decays to products which only contains π^0 , and the respective ratio of each channel is not changed.

$$\begin{aligned} D_{s1}^- (2460) &\rightarrow \pi^0 D_s^{*-} \quad B = 0.96 \\ &\rightarrow \pi^0 \pi^0 D_s^- \quad B = 0.04 \end{aligned} \tag{3}$$

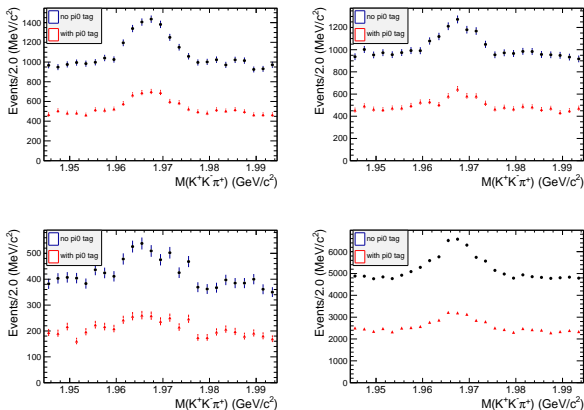
π^0 Tag

Figure: The entire D_s invariant mass spectrum with and without π^0 tag, for data at 4.467 GeV (upper left), 4.527 GeV (upper right), 4.575 GeV (lower left) and 4.600 GeV (lower right).

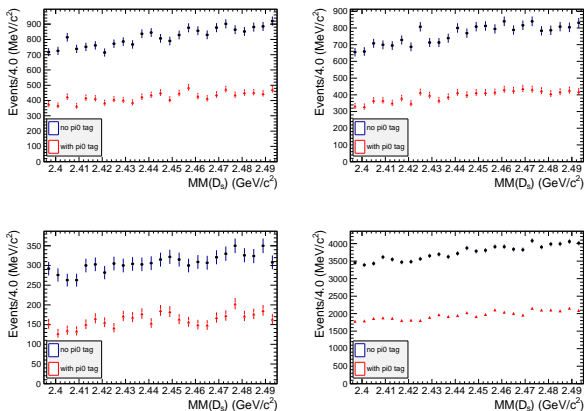
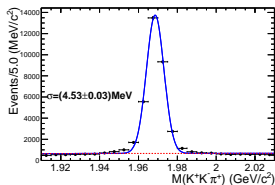
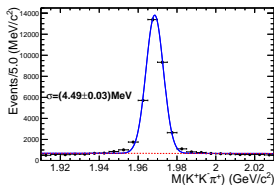
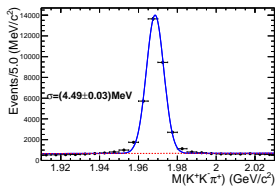
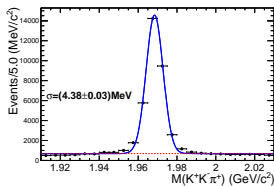
π^0 Tag

Figure: The D_s recoil mass spectrum with and without π^0 tag, for data at 4.467 GeV(upper left), 4.527 GeV(upper right), 4.575 GeV(lower left) and 4.600 GeV(lower right).

Fit of MC with π^0 Tag

Use the same procedure as we did without π^0 tag. First, Fit the entire D_s invariant mass spectrum.



Fit of MC with π^0 Tag

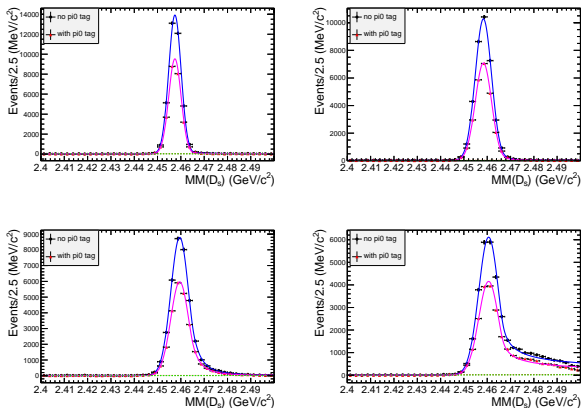
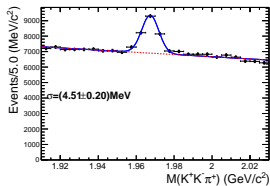
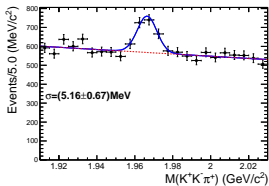
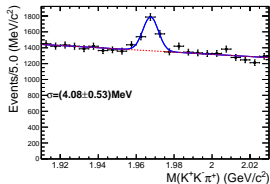
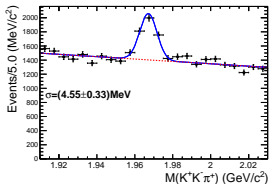


Figure: Fit in each bin to get the real D_s event count, and then fit the D_s recoil mass spectrum, with and without π^0 tag.

Fit of Data with π^0 Tag

Then, we perform the same fit for data.



Fit of Data with π^0 Tag

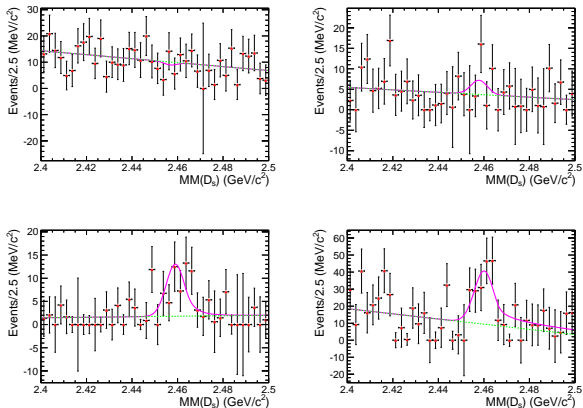


Figure: Fit in each bin to get the real D_s event count, and then fit the D_s recoil mass spectrum, with and without π^0 tag.

Fit Result

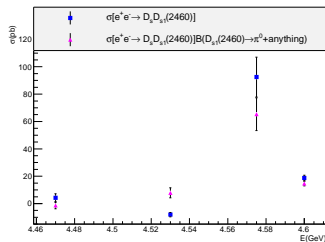
center-of-mass energy	efficiency	N_{event}	$(1 + \delta)^{ISR}$	significance
4.467	28.9%	-3.3 ± 6.1	1.035	—
4.527	28.6%	12.7 ± 5.9	0.684	2.5σ
4.575	24.6%	49.3 ± 9.0	0.706	7.3σ
4.600	27.0%	185.39 ± 21.1	1.061	11.1σ

Table: N_{event} come from data fitting and efficiency come from MC simulation. Errors here are statistical only.

Born Cross Section

energy point	σ
4.467	$-1.3 \pm 2.5\text{pb}$
4.527	$7.9 \pm 3.7\text{pb}$
4.575	$65.4 \pm 11.9\text{pb}$
4.600	$14.7 \pm 1.7\text{pb}$

Table: Born cross section of $e^+e^- \rightarrow D_s D_{s1}(2460), D_{s1}(2460) \rightarrow \pi^0 + \text{anything}$ calculated at four energy point



Branch Fraction

So, we can obtain $B(D_{s1}(2460) \rightarrow \pi^0 + \text{anything})$ by dividing $\sigma[e^+e^- \rightarrow D_s D_{s1}(2460), D_{s1}(2460) \rightarrow \pi^0 + \text{anything}]$ by $\sigma[e^+e^- \rightarrow D_s D_{s1}(2460)]$.

energy point	$B(D_{s1}(2460) \rightarrow \pi^0 + \text{anything})$
4.575	$(70.7 \pm 17.0)\%$
4.600	$(78.3 \pm 12.0)\%$

$$e^+ e^- \rightarrow D_s^{*+} D_{s1}^- (2460) + c.c.$$

Special Event Selection

Require at least three good charged tracks and one good photon. Perform a vertex fit on $K^+ K^- \pi^+$, then a two-constraint (2C) kinematic fit, with the mass constraints of D_s and D_s^* .

$$e^+ e^- \rightarrow D_s^{*+} D_{s1}^- (2460) + c.c.$$

Special Event Selection

Require at least three good charged tracks and one good photon. Perform a vertex fit on $K^+ K^- \pi^+$, then a two-constraint (2C) kinematic fit, with the mass constraints of D_s and D_s^* .

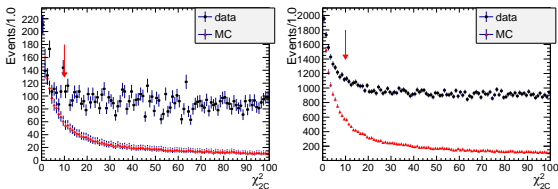


Figure: 4.575 GeV(left) and 4.6 GeV(right).

Here MC simulation is normalized to data with event in the first bin being the same.

Optimize the χ^2 cut

Optimized by FOM value: $\frac{s}{\sqrt{s+B}}$

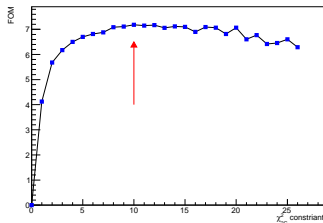
s : expected observed event,

$$s = \sigma * (1 + \delta)^{VP} * \varepsilon_{D_s^*} * B(D_s^* \rightarrow \gamma D_s) * B(D_s \rightarrow K^+ K^- \pi) * L * (1 + \delta)^{ISR}$$

the σ comes from rough measurement of the cross section at $\sqrt{s} = 4.575$ GeV: $24 pb$;

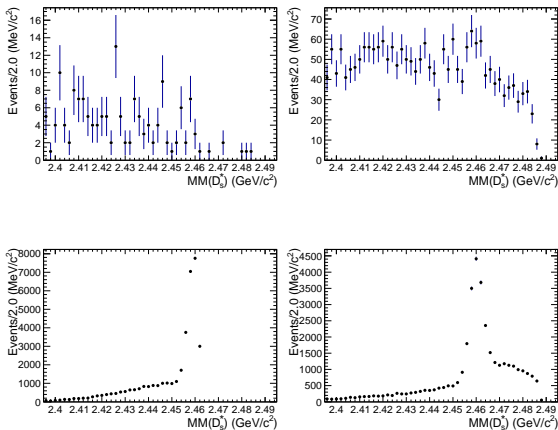
$\varepsilon_{D_s^*}$: the efficiency under variant χ_{2C}^2 constraint.

B : the background event count from inclusive MC sample in the D_s^* signal range.



Distribution

The distribution of $MM(D_s^*)$ for data(above) and MC(below), at 4.575 GeV(left) and 4.6 GeV(right).



Inclusive MC sample

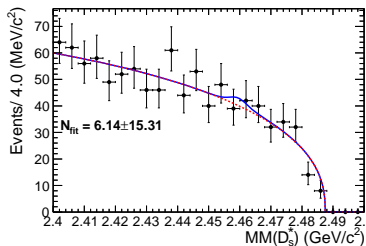


Figure: The distribution of $MM(D_s^*)$ for inclusive MC sample at $\sqrt{s} = 4.6$ GeV.

Background for $e^+e^- \rightarrow D_s^+ D_{s1}^- (2460)$

Potential backgrounds are listed below:

index	event tree	nEvts
1	$e^+e^- \rightarrow \pi^+ D^- D^{*0}, D^- \rightarrow \pi^0 \pi^- K^+ K^-, D^{*0} \rightarrow D^0 \gamma, D^0 \rightarrow \pi^0 \pi^+ K^-$	2
2	$e^+e^- \rightarrow \pi^+ \bar{D}^{*-} D^0, \bar{D}^{*-} \rightarrow \pi^- \bar{D}^0, D^0 \rightarrow \pi^0 \pi^+ K^-, \bar{D}^0 \rightarrow K^+ a_1^-, a_1^- \rightarrow \rho^0 \rho^-, \rho^- \rightarrow \pi^0 \pi^-$	2
3	$e^+e^- \rightarrow \pi^- D^+ \bar{D}^{*0}, D^+ \rightarrow \pi^+ \pi^+ K^-, \bar{D}^{*0} \rightarrow \pi^0 \bar{D}^0, \bar{D}^0 \rightarrow \pi^- \omega K^+, \omega \rightarrow \pi^0 \pi^+ \pi^-$	2
4	$e^+e^- \rightarrow \pi^+ \bar{D}^{*-} D^0, \bar{D}^{*-} \rightarrow \pi^- \bar{D}^0, D^0 \rightarrow K^- a_1^+, \bar{D}^0 \rightarrow e^- \bar{\nu}_e K^{*+}, a_1^+ \rightarrow \rho^0 \pi^+, K^{*+} \rightarrow \pi^0 K^+, \rho^0 \rightarrow \pi^+ \pi^-$	2
5	$e^+e^- \rightarrow \pi^0 D^{*0} \bar{D}^{*0}, D^{*0} \rightarrow \pi^0 D^0, \bar{D}^{*0} \rightarrow \bar{D}^0 \gamma, D^0 \rightarrow K^- a_1^+, \bar{D}^0 \rightarrow K^+ a_1^-, a_1^+ \rightarrow \rho^0 \pi^+, a_1^- \rightarrow \pi^0 \rho^-, \rho^0 \rightarrow \pi^+ \pi^-, \rho^- \rightarrow \pi^0 \pi^-$	2
6	$e^+e^- \rightarrow D^- D^{*+}, D^- \rightarrow \pi^- \pi^- K^+, D^{*+} \rightarrow \pi^+ D^0, D^0 \rightarrow \pi^0 \pi^+ K^-$	2
7	$e^+e^- \rightarrow D^{*0} \bar{D}^{*0}, D^{*0} \rightarrow D^0 \gamma, \bar{D}^{*0} \rightarrow \pi^0 \bar{D}^0, D^0 \rightarrow K^- a_1^+, \bar{D}^0 \rightarrow K^0 \phi, a_1^+ \rightarrow \rho^0 \pi^+, K^0 \rightarrow K_L, \phi \rightarrow K^+ K^-, \rho^0 \rightarrow \pi^+ \pi^-$	2
8	$e^+e^- \rightarrow \pi^0 D^{*0} \bar{D}^{*0}, D^{*0} \rightarrow D^0 \gamma, \bar{D}^{*0} \rightarrow \bar{D}^0 \gamma, D^0 \rightarrow K^- a_1^+, \bar{D}^0 \rightarrow K^+ a_1^-, a_1^+ \rightarrow \pi^0 \rho^+, a_1^- \rightarrow \rho^0 \pi^-, \rho^+ \rightarrow \pi^0 \pi^+, \rho^0 \rightarrow \pi^+ \pi^-$	1
9	$e^+e^- \rightarrow \bar{D}^0 D^{*0}, \bar{D}^0 \rightarrow \mu^- \bar{\nu}_\mu K^{*+}, D^{*0} \rightarrow \pi^0 D^0, K^{*+} \rightarrow \pi^0 K^+, D^0 \rightarrow K^- a_1^+, a_1^+ \rightarrow \rho^0 \pi^+, \rho^0 \rightarrow \pi^+ \pi^-$	1
10	$e^+e^- \rightarrow \pi^- D^{*+} \bar{D}^{*0}, D^{*+} \rightarrow \pi^+ D^0, \bar{D}^{*0} \rightarrow \bar{D}^0 \gamma, D^0 \rightarrow K^- a_0^+, \bar{D}^0 \rightarrow \rho^0 K^*, a_0^+ \rightarrow \pi^+ \eta, \rho^0 \rightarrow \pi^+ \pi^-, K^* \rightarrow \pi^- K^+, \eta \rightarrow \pi^0 \pi^0 \pi^0$	1
11	$e^+e^- \rightarrow D^{*0} \bar{D}^{*0}, D^{*0} \rightarrow \pi^0 D^0, \bar{D}^{*0} \rightarrow \pi^0 \bar{D}^0, D^0 \rightarrow \pi^0 \pi^0 K^+ K^-, \bar{D}^0 \rightarrow \pi^0 \pi^+ \pi^- K^*, K^* \rightarrow \pi^0 K^0, K^0 \rightarrow K_S, K_S \rightarrow \pi^+ \pi^-$	1
12	$e^+e^- \rightarrow D^{*0} \bar{D}^{*0}, D^{*0} \rightarrow \pi^0 D^0, \bar{D}^{*0} \rightarrow \bar{D}^0 \gamma, D^0 \rightarrow \pi^0 \pi^+ K^-, \bar{D}^0 \rightarrow \pi^- \bar{K}^0 K^+, \bar{K}^0 \rightarrow K_S, K_S \rightarrow \pi^+ \pi^-$	1
13	$e^+e^- \rightarrow \pi^+ \bar{D}^{*-} D^{*0}, \bar{D}^{*-} \rightarrow \pi^- \bar{D}^0, D^{*0} \rightarrow \pi^0 D^0, \bar{D}^0 \rightarrow \pi^0 \pi^- K^+, D^0 \rightarrow \pi^0 \pi^+ K^0 K^-, K^0 \rightarrow K_L$	1

Fit of MC

Argus for background, Crystal ball for signal.

The cross section used for computing Initial State Radiation(ISR) is the same as that in $e^+e^- \rightarrow D_s^+ D_{s1}^- (2460)$.

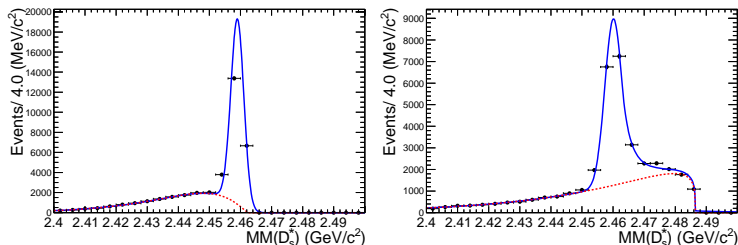


Figure: Fit of the recoil mass distribution of D_s^* for MC simulation, at 4.575 GeV(left) and 4.6 GeV(right).

Fit of Data

Crystal ball convolve Gaussian for signal, where the Gaussian function represents the difference between data and MC on resolution and its σ is fixed to 0.9 MeV.

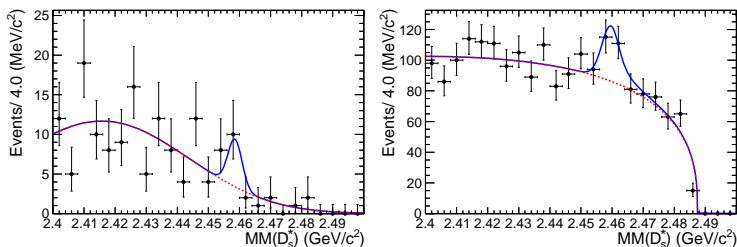


Figure: Fit of the recoil mass distribution of D_s^* for data at 4.575 GeV (left) and 4.6 GeV (right).

Fit Result

center-of-mass energy	efficiency	N_{event}	$(1 + \delta)$	significance
4.575	19.7%	9.07 ± 3.91	0.709	2.8σ
4.600	15.8%	77.7 ± 22.8	1.060	3.4σ

Table: N_{event} come from data fitting and efficiency come from MC simulation. Errors here are statistical only.

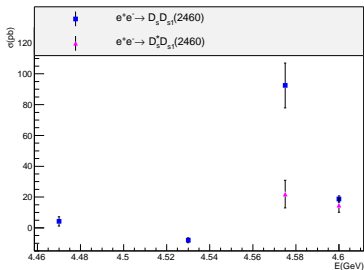
Born Cross Section










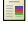

$$\sigma = \frac{N_{obs}}{(1 + \delta)^{VP} * \epsilon_{D_s^*} * B(D_s^* \rightarrow \gamma D_s) * B(D_s \rightarrow K^+ K^- \pi) * L * (1 + \delta)^{ISR}} \quad (4)$$

energy point	σ
4.575	$24.6 \pm 10.6\text{pb}$
4.600	$14.7 \pm 4.5\text{pb}$

Summary

- 1 Measured the born cross section of $e^+e^- \rightarrow D_s D_{s1}(2460)$ at 4 energy points, and $e^+e^- \rightarrow D_s^* D_{s1}(2460)$ at 2 energy points.
- 2 Systematic uncertainty in progress.
- 3 Not consistent with the prediction[8].



-  D. Besson *et al.*, CLEO Collaboration, Phys. Rev. D **68** (2003) 032002.
-  P. Krokovny *et al.*, Belle Collaboration, Phys. Rev. Lett. **91** (2003) 262002.
-  M. Bondioli, BaBar Collaboration, Nucl. Phys. B (Proc. Suppl.) **133** (2004) 158.
-  F. A. *et al.*, Phys. Rev. D **76** (2007) 114008.
-  M. Cleven *et al.*, Eur. Phys. J. A **50** (2014) 149.
-  C. J. Xiao *et al.*, Phys. Rev. D **93** (2016) 094011.
-  P. G. Ortega *et al.*, EPJ Web Conf. **130** (2016) 02009.
-  M. Voloshin, arXiv:1802.09492 [hep-ph].
-  C. Hua-Xing *et al.*, Reports on Progress in Physics **80** (2017) 076201.
-  P. C. *et al.*, Particle Data Group Collaboration, Chin. Phys. C **40** (2016) 100001.
-  X. working group, *XYZProposal*,
<http://docbes3.ihep.ac.cn/~charmoniumgroup/index.php/XYZProposal>.

$$e^+e^- \rightarrow D_s^+ D_{s1}^- (2460)$$

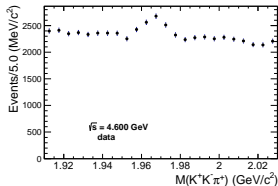
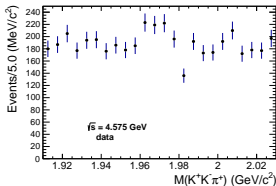
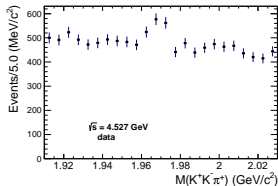
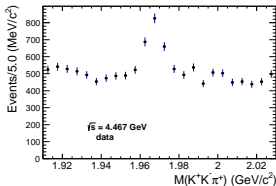


Figure: The distribution of $M(K^+K^-\pi^+)$ with the constraint of $MM(D_s)$ in the range of $[2.4, 2.5]$, for data.

Background for $e^+e^- \rightarrow D_s^+ D_{s1}^-$ (2460)

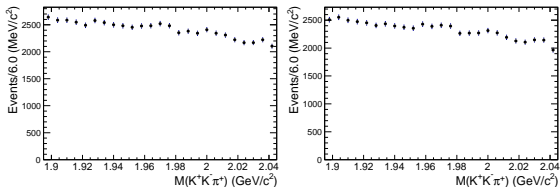


Figure: The D_s spectrum with $MM(D_s)$ in range [2.4, 2.5], for inclusive MC simulation at 4.575 GeV(left) and 4.600 GeV(right).

